Optica Applicata, Vol. XXX, No. 1, 2000

Investigation of dynamic and stability of laser-produced plasma in strong external magnetic field

TADEUSZ PISARCZYK, ANDRZEJ KASPERCZUK, RYSZARD MIKLASZEWSKI

Institute of Plasma Physics and Laser Microfusion, ul. Hery 23, 00–908, Warszawa, Poland.

YURI P. ZAKHAROV

Institute of Laser Physics RAS, Pr. Lavrentyeva 13/3, Novosibirsk, 630090, Russia.

The paper presents results of studies of the behaviour of a laser-produced plasma in strong external axial and transverse magnetic field of 5–20 T in induction generated from a flat teflon target at the laser power densities of about 10^{14} Wcm^{-2}. The investigations were carried on by means of a three-frame interferometry and a non-contact magnetic probe, so-called remote magnetic probe (RMP). The dyamics of the process of creation of the diamagnetic cavity, its shape and dimensions have been determined. Also computer simulation of plasma expansion by 2D MHD code was made.

1. Indroduction

The behaviour of plasma streams, produced at irradiation of targets made from various-Z materials by intense laser radiation, in external magnetic field has been the subject of studies at numerous laboratories in the world many years. Taking into account the maximum attainable value of the magnetic field induction, its distribution, power density of laser radiation as well as the apparatus for plasma diagnostics, these studies comprise such research aspects as: magnetic confinement of a thermonuclear plasma, modelling of solar wind interaction with magnetosphere, and formation of a plasma column with magnetic field to obtain optimum conditions for X-ray lasing [1]–[3]. In spite of great efforts of experimenters, the mechanisms of laser plasma interaction with magnetic field have not been well understood so far. Due to an angular character of laser-plasma expansion (which is related to the manner of its production by focusing a laser beam) and the occurrence of numerous physical effects accompanying laser beam interaction with a target (*e.g.*, a shock wave, heat conduction or XUV radiation), mathematical modelling of plasma behaviour in external magnetic fields as well as the diagnostics of such a plasma are very complex. It should be noted that in the case of axial magnetic fields (with direction of field lines corresponding to direction of the laser beam) expansion of plasma is axially symmetrical in principle, whereas in the case of fields with the

geometry different from axial this symmetry can be strongly disturbed. This sets a requirement that tomographic disgnostics be used [4], [5] for measuring spatial distributions of parameters of such a plasma, whereas for the modelling of plasma three-dimensional codes are required.

Most of the studies in this field, however, deal with interaction of a laser plasma with relatively weak magnetic fields the induction of which does not exceed 1 T. In this work, in contradistinction to others, we present results of investigations and analysis of laser-produced plasma interaction with strong axial and transverse magnetic fields of 5–20 T in amplitude. We attempt at summarising the studies of a laser-produced plasma in strong magnetic field we have carried out for the last few years [6]–[9].

2. Investigation of laser-produced plasma in strong axial magnetic field

The plasma was produced by focusing a Nd-laser beam, with the pulse parameters $E_l \approx 10$ J and $\tau \approx 1$ ns, by means of a lens of the focal length $f = 180$ mm on a flat target made from teflon. The target was placed on the axis of a one-turn coil enabling the magnetic field of up to 20 T in amplitude to be obtained. The spatial and temporal measurements of distributions of electron concentration were carried on by means of an automated three-channel interferometer described in [10]. The experimental setup [7] enabled observation of a plasma column produced in magnetic field in a temporal range from 0 to even a few tens of nanoseconds counting from the moment of incidence of the main laser pulse on the target. To inspect the influence of magnetic field on the plasma and to determine essential differences in the case of $B_0 \neq 0$ in subsequent phases of this process, it was indispensable to get to know deeply the course of the process of free expansion of the laser plasma (at $B_0 = 0$). Detailed interferometric investigations of this process have demonstrated that one can distinguish two components in the plasma: fast and slow. The fast component occurs in the initial phase of the process and corresponds to a thermal plasma produced as a result of ablation of the target's material. The front of the fast plasma propagates with the axial speed $V_z \approx 3 \cdot 10^7$ cm/s. After its decay ($t > 15$ ns) the slow component of the plasma appears having the axial speed one order of magnitude lower than the fast component. The slow component is constituted by a plasma generated from the crater created in the target as a result of secondary processes accompanying generation of the laser-produced plasma such as: shock wave, heat conduction, and XUV radiation. The character of the slow plasma outflow is strictly related to the character of expansion of the ablative plasma. The existence of the fast and slow components is confirmed by the linear electron density distributions and the total number of electrons, as shown in Fig. 1.

Among the cases of plasma expansion analysed, one can distinguish two essentially different kinds of geometry of plasma expansion: angular and axial expansion. The isodensitograms for both kinds of expansion are shown in Fig. 2. Angular expansion (Fig. 2a) is characterized by distinct angular emission of plasma with respect to the axis and by the occurrence of a distinct minimum in the dis-

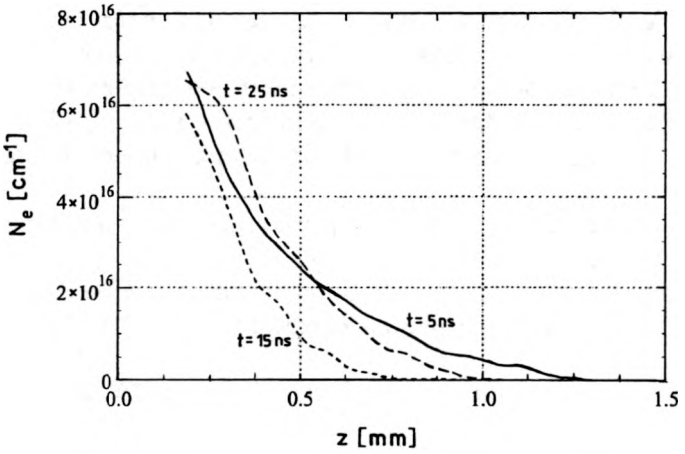

Fig. 1. Linear electron density distribution for the free expansion of the laser-produced plasma. $t = 5$ ns: $N = 1.97 \times 10^{15}$; $t = 15$ ns: $N = 10.8 \times 10^{15}$; $t = 25$ ns: $N = 1.88 \times 10^{15}$ (N — total number of electrons).

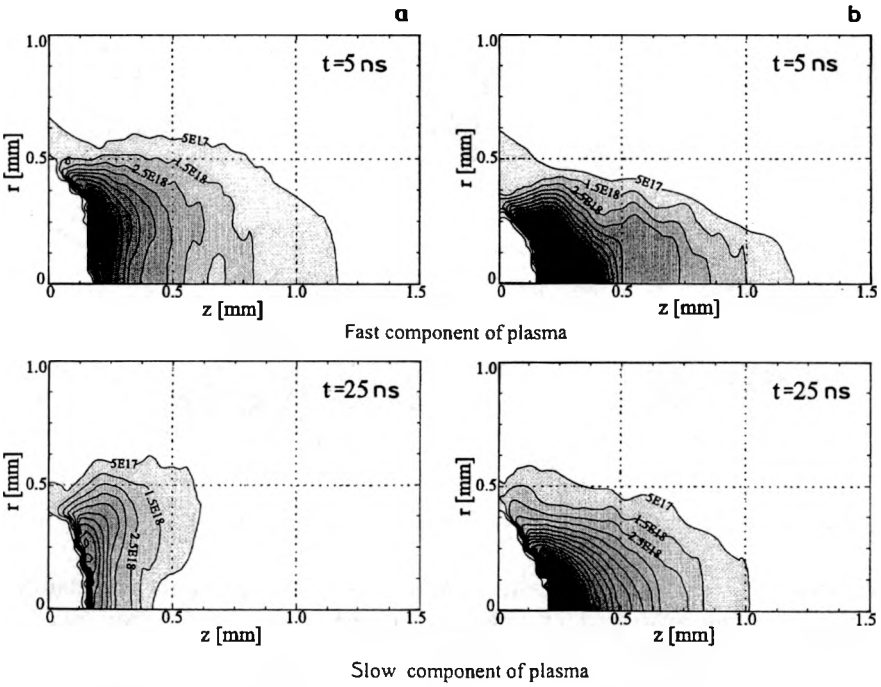

Fig. 2. Free expansion of laser-produced plasma: **a** — angular expansion, **b** — axial expansion.

tribution of the plasma electron concentration visible practically in the whole range of expansion times observed. In the case of axial expansion of the plasma (Fig. 2**b**), we can observe decidedly axial motion of the plasma. The front of outflow of the slow component has the shape of a paraboloid of revolution directed with its apex

towards the direction of propagation. In contradistinction to the angular regime, the axial distribution of electron concentration has its maximum on the axis. The regimes of expansion are described in detail in [7]. The interferometric measurements of a laser-produced plasma in external magnetic field in the range 5–20 T enabled us to distinguish the following characteristic phases of development of this phenomenon:

– the phase of radial expansion of the plasma (comprising the time range from the moment of plasma creation to $t = 5$ ns),

– the phase of radial implosion of the plasma occurring at $t = (5-15)$ ns,

– the phase of radial reexpansion of the plasma corresponding to expansion times $t = (15-25)$ ns,

– the phase of disintegration of the plasma beginning from $t > 25$ ns.

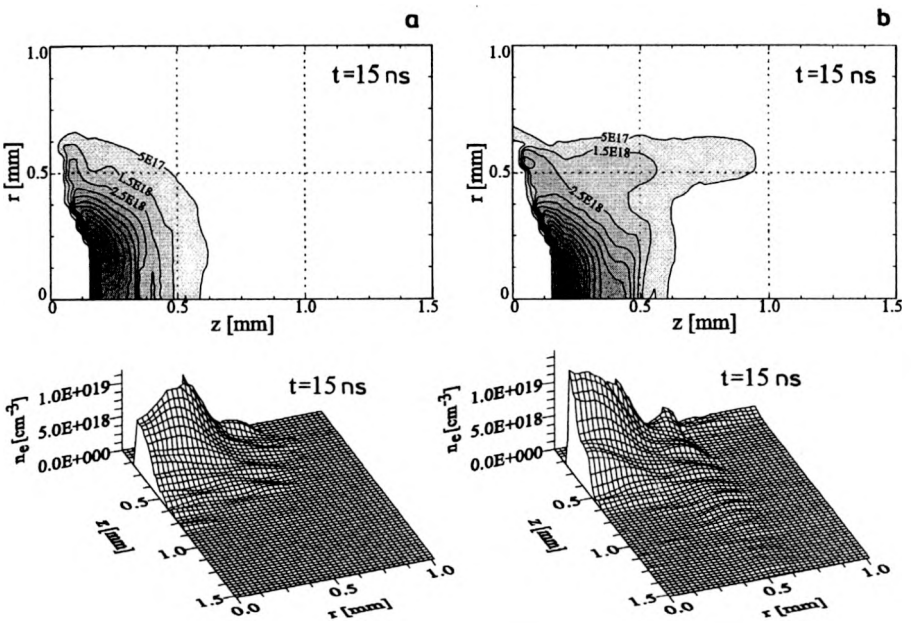

Fig. 3. Electron density distributions in the phase of radial implosion: **a** – $B_0 = 0$, **b** – $B_0 = 10$ T.

During the first five nanoseconds, in the phase of radial expansion, one cannot observe in interferograms any distinct influence of the magnetic field on plasma expansion. Essential differences, in comparison with free expansion, emerge after subsequent 10 ns, in the phase of radial implosion (Fig. 3), beginning at the moment of reaching a maximum radius by the plasma. In this phase, the shape of the front of expanding plasma changes. The flat front, occurring in the absence of magnetic field (Fig. 3a) changes decidely into a concave one (Fig. 3b) at $t = 15$ ns. This is related to the emergence of additional wings of about 0.5 mm in length at the plasma front. These wings are created by a plasma of relatively low electron concentration, $n_e < 10^{18}$ cm^{-3}. As a result of radial implosion, an intense axial outflow (cumulative

stream) emerges, the start of which is apparent in Fig. 3**b** in the form of a jump in electron concentration at the plasma front. This jump is distinctly apparent in the next phase of the phenomenon (Fig. 4).

In general, the plasma stream induced by implosion of the axially symmetrical plasma sheath has a lenghtened shape and a speed considerably higher than the speed of the edge of the imploding sheath (here, about $2 \cdot 10^6$ cm/s). Due to the fact that in our case this stream has a decidedly flat front and a low speed on the axis ($\sim 1.5 \cdot 10^6$ cm/s), in the next phase of development of the phenomenon, *i.e.*, reexpansion (Fig. 4), one can observe strong radial spread of the stream along the concave front of expanding plasma formed earlier, due to which concentration of the plasma in the wings increases several times.

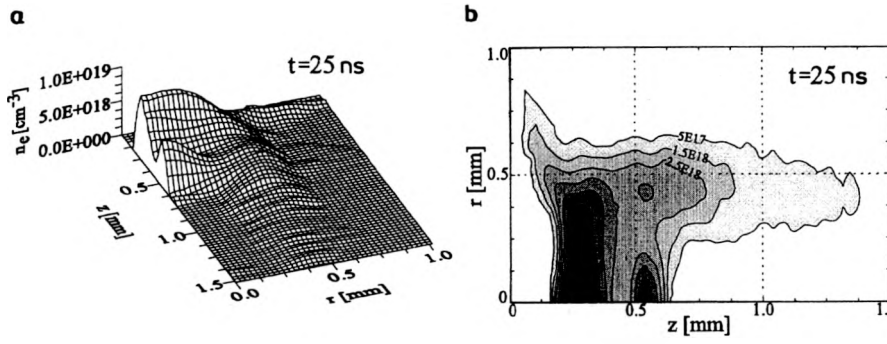

Fig. 4. Electron density distributions in the phase of radial reexpansion: **a** — spatial profile of electron density distribution, **b** — isodensitogram.

The plasma concentration in the wings at the end of the reexpansion phase amounts to $n_e = 4 \cdot 10^{18}$ cm^{-3}. The wings precede the plasma front on the axis, the result of which is that the axial motion of the whole plasma in the stream is faster than the motion of the stream on the axis. The radial flow of the stream induced by implosion towards the wings together with reexpansion of the plasma cause that most of the plasma at $t = 35$ ns (Fig. 5**a**) is located outside the axis. In the final stage of development of the phenomenon, at the moment when the source of plasma gets exhausted, only the outer plasma remains having the maximum electron concentration of about $2 \cdot 10^{18}$ cm^{-3}, and the shape of a hollow cylinder. This correspond to the situation presented in Fig. 5**b** ($t = 45$ ns). The length of this cylindrical configuration corresponds to the range of the wings, while its internal diameter is about 0.5 mm.

In the case of axial expansion, the influence of magnetic field on the course of the phenomenon is observed as late as after 15 ns from the moment of plasma generation. The differences, in comparison with free expansion, relate mainly to the disturbance of outer regions of the plasma cloud formed being in close contact with the axial magnetic field. After $t = 15$ ns, characteristic wings ("arms") of thin plasma also appear, which are about twice as long in this case as those for angular emission.

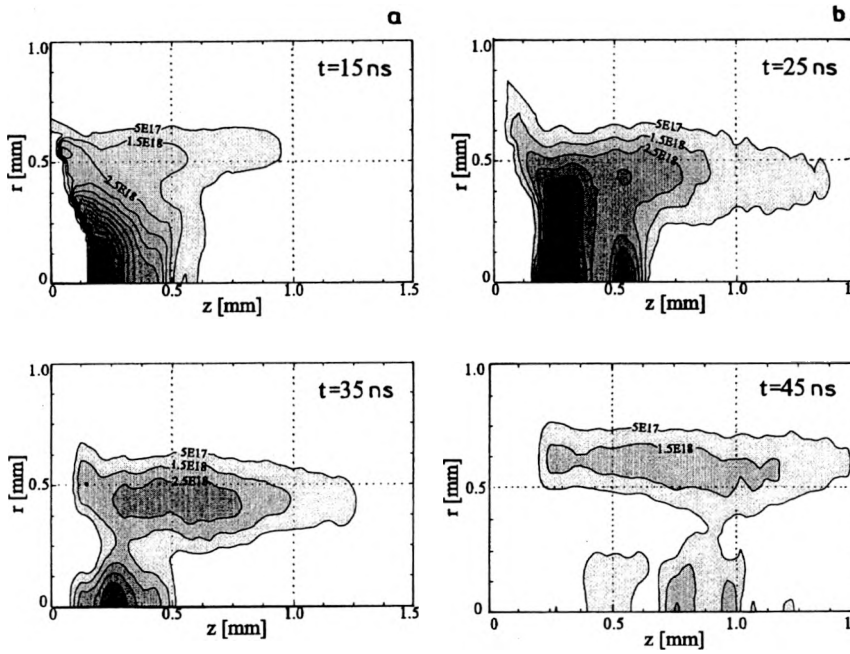

Fig. 5. Formation of cylindrical configuration of plasma in the late phase of expansion.

Analyzing the distributions of electron concentration obtained, it has been proved that partial outflow of the plasma to the wings does not influence strongly the behaviour of the central dense plasma corresponding to the slow component of the plasma. The slow component, as in the case of free expansion, has the shape of a paraboloid of revolution with a characteristic maximum of electron concentration remaining on the axis during the whole process.

The differences presented above in the behaviour of plasma in magnetic field in respect to free expansion enabled us to make a phenomenologic description of mutual plasma-magnetic-field interaction. Characteristic variations in the motion of the slow component of plasma can be induced only by deformation of magnetic field by the fast component of plasma. Thus, at the moment of plasma emergence on the surface of the target, magnetic-field lines become frozen in the plasma (the diffusion time of magnetic field at a temperature of merely a few electron-volts exceeds the time scale of the phenomenon under study). The fast plasma, expanding at large angles with respect to the axis, carries magnetic-field lines deforming its distribution and producing so-called diamagnetic cavity of the radius $R_B \sim B_0^{-2/3}$. The distribution of magnetic-field lines, deformed during the process of diamagnetic-cavity creation, enforces the flow of the slow component in further phases of the phenomenon adequate to the regime of plasma expansion [7]. To model the behaviour of plasma in axial magnetic field, a 2D MHD model described in [8] was developed. The numerical modelling has shown that the factor responsible for the occurrence of a specific regime is the distribution of intensity of laser radiation on the target. The angular regime occurs when the target is illuminated by laser radiation

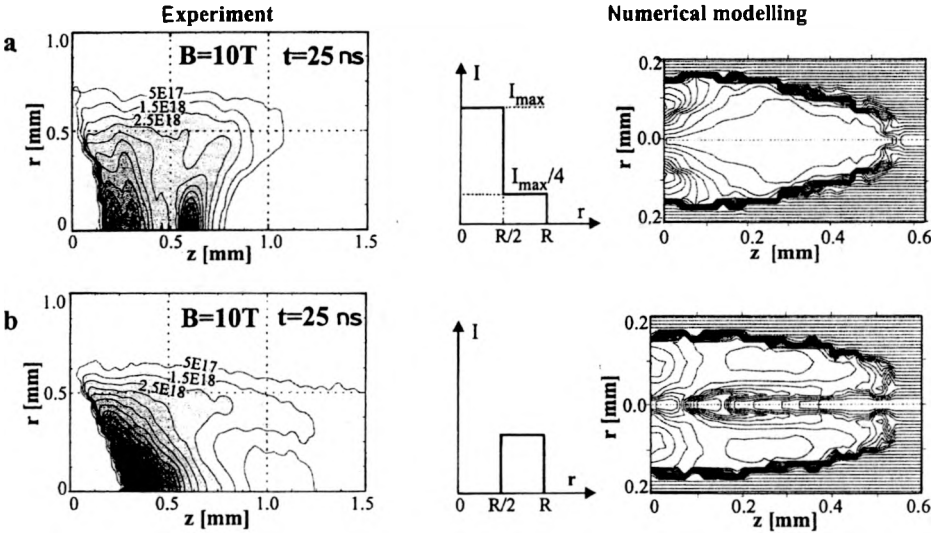

Fig. 6. Results of numerical modelling of plasma in magnetic field for: **a** — angular expansion, **b** — axial expansion.

the distribution of which has a maximum of intensity on the axis (Fig. 6**a**), whereas axial expansion takes place when the intensity distribution is reverse, *i.e.*, with a minimum on the axis (Fig. 6**b**). The 2D modelling has also proved that the definite deformation of the magnetic-field distribution by the ablative plasma, responsible for the enforcement of flow of the slow component of plasma, occurs very rapidly (for $t \leqslant 1$ ns). This is proved by the phenomenological image of the phenomenon course presented above. Our investigations show that, in axial magnetic field, it is practically impossible to generate a relatively homogeneous stream of a laser-produced plasma in the early phase of plasma expansion, which stream could be the medium of an X-ray laser. However, it is interesting in this context that a plasma cylinder is created in the final stage of evolution which can constitute an advantageous configuration for propagation and amplification of coherent X-rays.

3. Investigations of laser-produced plasma in transverse magnetic field

The behaviour of a laser-produced plasma in strong external tranverse magnetic field of above 10 T in induction generated from a flat teflon target at the laser power densities of about 10^{14} Wcm^{-2} was investigated. In the measurements of plasma parameters, a two-channel automated interferometric system [9], [10] and a RMP method (elaborated by ZAKHAROV [11]) were used. For the needs of these investigations we developed:

— a tomographic method for reconstruction of asymmetrical electron density distribution in the diamagnetic cavity,

— a methodology for measuring the dimensions of the cavity during its expansion by means of the RMP.

To measure the amplitude of the magnetic field a magnetic probe was used. Experimental setup is described in papers [9], [11].

3.1. Determination of spatial distribution of electron density in a plasma stream of disturbed axial symmetry

In the studies of a laser-produced plasma, we usually deal with a plasma having axial symmetry [12]. In such a case, it is sufficient to probe the plasma in one direction perpendicular to its axis of symmetry to determine the spatial distribution of electron density n_e. The change in phase S, determined by means of interferometry, induced by the presence of the plasma, is related to n_e by the known Abel equation of the form

$$S(y) = 8.92 \cdot 10^{-14} \lambda \int_y^R \frac{n_e(r) r dr}{\sqrt{r^2 - y^2}} \tag{1}$$

where the quantities y, r and R are defined in Fig. 7, λ is the wavelength in centimeters, and n_e is given in cm^{-3}.

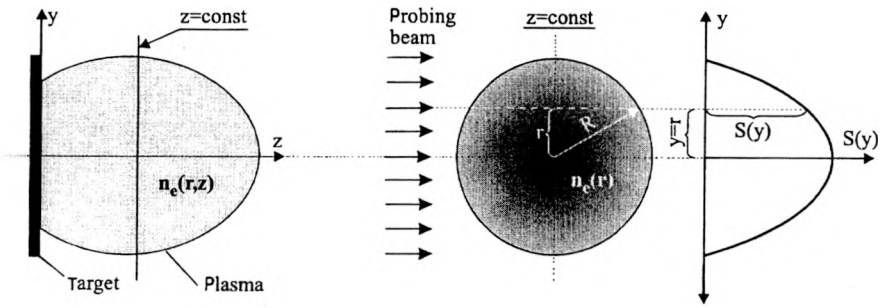

Fig. 7. Geometric interpretation of the Abel integral equation.

When the plasma under investigation differs considerably from symmetrical one by its nature, it is indispensable to apply a tomographic interferometry. This is connected with the necessity of probing the plasma in a few directions simultaneously. The number of directions for probing the plasma and their orientation are commonly determined by actual experimental conditions.

In our experiment, due to a limited access to the plasma located inside the magnetic coil, it was possible to probe the plasma in two directions only. For this reason, application of the methods proposed in literature [5], [13], based on expansion of the S and n_e functions in a Fourier series, did not give correct results. Therefore, to reconstruct spatial distributions of n_e, we applied a methodology developed for the experiment under consideration.

It should be emphasized that the plasma stream that we investigated, initially symmetrical, underwent deformation only in the front layer ($z > 0.4$ mm). Along its total length, the plasma stream kept approximately a circular cross-section, while

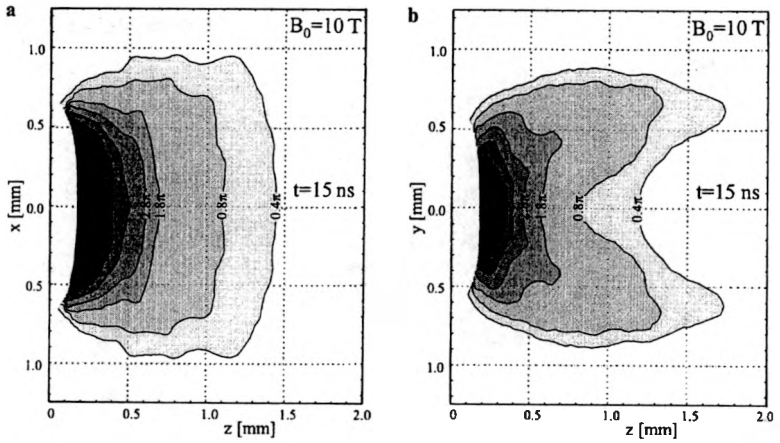

Fig. 8. Samples of phase distributions corresponding with the plasma of disturbed axial symmetry registered perpendicularly (a) and parallely (b) to the magnetic-field direction.

the axial unsymmetrical part of the plasma was characterized by symmetry with respect to the xz and yz planes (Fig. 8). This justifies the assumption that the distribution of n_e is a superposition of two distributions: axially symmetrical and asymmetrical.

Shining through the plasma in two directions, parallel ($\parallel$) and perpendicular ($\perp$) to the magnetic-field lines (Fig. 9), we obtained two distributions, $S_{\parallel}(x)$ and $S_{\perp}(y)$ for each cross-section parallel to the target surface. Then, we assumed that $S_{\parallel}(x) = S_0(x) + S_1(x)$, where $S_0(x)$ corresponded with the part of the plasma having axial symmetry, while $S_1(x)$ — with the asymmetrical part of the plasma.

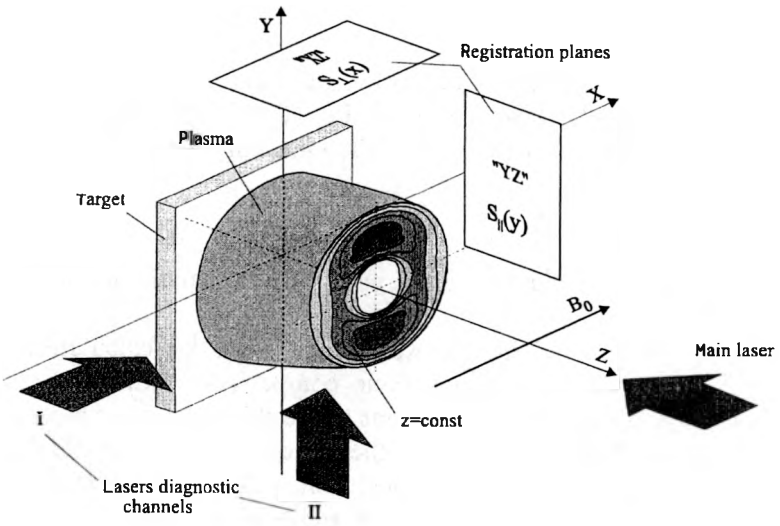

Fig. 9. Method of probing the plasma having symmetry with respect to the xz and yz plsnes for reconstruction of electron density spatial distribution.

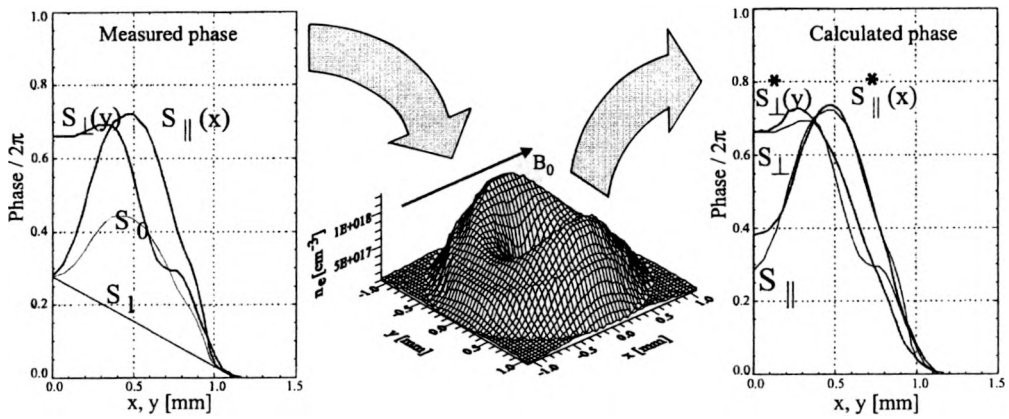

Fig. 10. Illustration of the methodology for reconstruction of electron-density spatial distribution and checking correctness of calculations. The calculations have been performed for the following values of the matching coefficients: $A_0 = 1.0$, $A_1 = 0.7$.

In order to determine the function $S_0(x)$, the points $S_\parallel(0)$ and $S_\parallel(R)$ were connected (see Fig. 10) and a straight line was obtained which can be expressed by the formula

$$S_l(x) = -\frac{S_\parallel(0)}{R}x + S_\parallel(0). \tag{2}$$

The functions $S_0(x)$ and $S_1(x)$ were determined from the following relations:

$$S_0(x) = \frac{S_\parallel(x) + S_l(x)}{2}, \tag{3}$$

$$S_1(x) = S_\parallel(x) - S_0(x). \tag{4}$$

The knowledge of functions $S_0(y)$ and $S_1(y)$ allowed the distributions $n_{e0}(r)$ and $n_{e1}(r)$ to be determined, respectively, with the use of Eq. (1). To express the spatial distribution of n_e in polar coordinates (r, θ), the following empirical formula was used:

$$n_e(r,\theta) = A_0 n_{e0}(r) + A_1 n_{e1}(r)(1 - \cos 2\theta) \tag{5}$$

where A_0 and A_1 are matching coefficients selected with the least-square method, the axis x corresponds to $\theta = 0$.

The distribution $n_e(r, \theta)$ calculated in this way was verified by calculation of corresponding distributions, $S_\parallel^*$ and $S_\perp^*$, and their comparison with the actual distributions. The coefficient A_0 was taken such that we could recover precisely the distribution $S_\perp$ near the axis of symmetry, *i.e.*, in the region where the asymmetric part of the plasma did not interfere, whereas the coefficient A_1 was to provide correct recovery of the distribution $S_\parallel$ and the remaining part of the distribution $S_\perp$. Proper selection of the parameters A_0 and A_1 allowed a relatively precise recovery of phase distributions (see Fig. 10) and, thereby, the distributions $n_e(r, \theta)$.

3.2. The "remote" magnetic probe (RMP) method

The method of magnetic probes is a well-known diagnostic technique for the measurement of plasma diamagnetism by registering a magnetic-field drop inside the plasma. However, interaction of a laser-produced plasma with a strong magnetic field is limited to very small dimensions of the order of 1 mm. In such a case, the common method (consisting in introduction of a probe to the plasma region) leads to disturbance of the plasma expansion process. Therefore, for the needs of this experiment, the RMP method has been applied.

The RMP measurement was accomplished by means of a three-turn magnetic probe of 2 mm in turn diameter. The probe was placed at a distance $r_p = 5$ mm from the target surface. Variations in the magnetic field, ΔB, in the probe surroundings were determined via usual electromagnetic induction law which, taking into account the finite probe size, leads to the following relation:

$$\Delta B = 1.7 \cdot 10^4 \int_0^t u_d \, dt \tag{6}$$

where: ΔB is expressed in Gs, $u_d \sim \partial B/\partial t$ is the voltage registered by the probe in μV, and t – the time measured from the moment of plasma generation in seconds. The quantity $\int_0^t u_d dt$ was registered directly by a Tektronix TDS 684A oscilloscope with digital integration.

In this case, a magnetic probe placed at a large distance from the plasma measures compression of the magnetic field ΔB^+ outside the expanding plasma (Fig. 11).

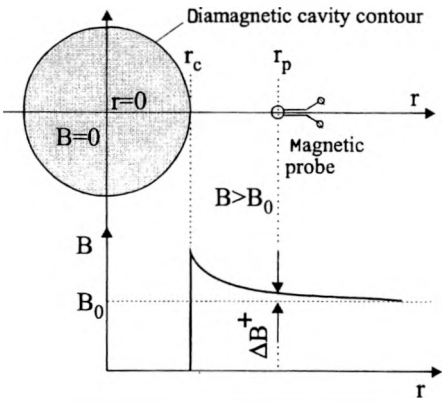

Fig. 11. Case of a spherically expanding plasma.

In the simplest ideal case, a superconducting sphere of the radius r_c, inside of which $B_0 = 0$, *i.e.*, $\Delta B^- = B_0$, causes disturbance of the field $\overline{\Delta B}$, in vacuum according to the dipole relation [14]

$$\overline{\Delta B} = 0.5\left(\frac{r_c}{r_p}\right)^3 \left[\bar{B}_0 - \frac{3(\bar{B}_0 \bar{r}_p)\bar{r}_p}{r_p^2}\right] \tag{7}$$

where $\bar{r}_p$ is the radius vector determining the position of the magnetic probe with respect to the centre of the sphere.

For the region close to the equatorial plane, where $\bar{r}_p \perp \bar{B}_0$, we have the following relation of r_c with the field compression ΔB^+:

$$r_c(t) = r_p \left[\frac{2\Delta B^+(t)}{B_0}\right]^{1/3}. \tag{8}$$

Due to the fact that, for such a case, the plasma of the kinetic energy E_k should be stopped by the field B_0 at a distance

$$R_B = \left(\frac{3E_k}{B_0^2}\right)^{1/3}, \tag{9}$$

hence $r_{c\max} \approx R_B$ (all values in Gaussian units).

Earlier investigations carried on with the RMP method for spherically expanding plasma at the KI-1 laser facility in Novosibirsk [15], [16], proved very good consistency of experimental results of both direct ($r_p < r_c$) and RMP ($r_p > r_c$) cavity measurements with relations (8) and (9), when the following condition is fulfilled:

$$\varepsilon_B = \frac{R_h}{R_B} \leqslant 1 \tag{10}$$

where R_h is the directed ion Larmor radius.

It is well known that, for flat targets, spatial distributions of the initial velocity of plasma expansion v_s, the ion current j and other parameters are functions of $\cos^\alpha \theta$, where θ is the angle between the normal to the target and the direction of plasma expansion.

Earlier measurements of the spatial distributions of v_s and j, performed for plastic target [17], have enabled us to determine the coefficients α for both these quantities: $\alpha \approx 1$ for v_s and $\alpha \approx 4$ for j. Thus, the spatial distribution of the plasma kinetic energy should have the form

$$\frac{dE_k}{d\Omega} \sim \cos^5 \theta. \tag{11}$$

It should be noticed that the relation

$$v_s = v_{s0} \cos\theta \tag{12}$$

describes spherical shape of both the plasma stream and its diamagnetic cavity (at a stage of $r_c \ll r_B$). The centre of this sphere lies in the middle of the axial dimension of the cavity ρ_{c0} corresponding to $\theta = 0$ (see Fig. 12). In the case under analysis, we may assume that the distribution of diamagnetic current on the surface of the plasma should be the same as in the case of "true" spherical expansion, therefore the disturbance of the magnetic field around the plasma can also be described by relations (7), (8). Considering the shift of the sphere centre by $\rho_{c0}/2$ from the target, we obtain the following expression for determination of dimensions of the diamag-

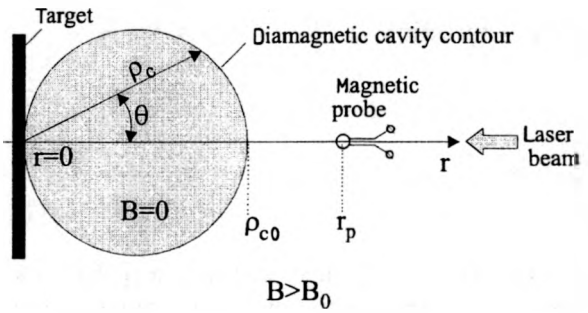

Fig. 12. Geometry of plasma expansion for flat target.

netic cavity ρ_{c0} with the RMP method

$$\rho_{c0}(t) = \frac{2r_p}{1+\left[\frac{B_0}{2\Delta B^+(t)}\right]^{1/3}}. \tag{13}$$

It should be noticed that for the angular distributions (11), (12) and at the plasma profile close to a uniform density, the spherical shape of diamagnetic cavity should be preserved till the stopping of the plasma by the magnetic field, *i.e.*, when $\rho_{c0} = \rho_{c0\,max} \approx R_B$.

Practical usage of relation (9) in the case of plasma expansion analyzed [18] requires replacement of E_k with another effective plasma kinetic energy E_e considered as equivalent value to the "true" sphere of the radius ρ_{c0} (Fig. 13). It is defined as follows:

$$E_e = 4\pi\left(\frac{dE_k}{d\Omega}\right)_{\theta=0}. \tag{14}$$

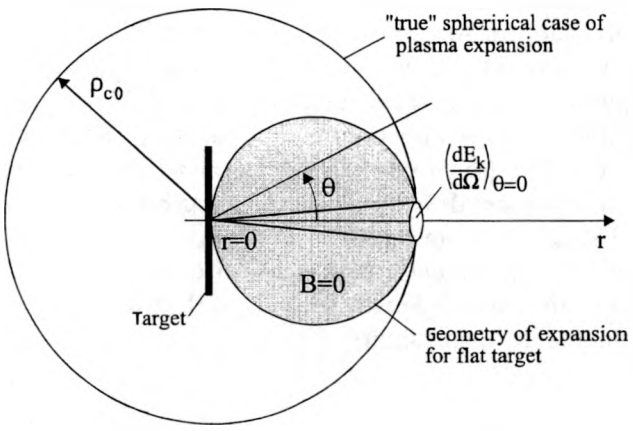

Fig. 13. Cases of plasma expansion considered and their mutual relations.

Applying relation (11), we obtain the expression

$$\frac{dE_k}{d\Omega} = \frac{E_e}{4\pi}\cos^5\theta, \tag{15}$$

which, after integration, gives the relation

$$E_e = 12E_k. \tag{16}$$

This way, analogous to the case of "true" spherical expansion [16], the knowledge of E_k (and vice versa) enables us to determine the maximum range of the diamagnetic cavity as $\rho_{c0\,\max} \approx R_B(E_e)$ for the case of directional expansion.

4. Results of investigation

The interferometric measurements accomplished in this work, as well as earlier investigations of the dynamics of a plasma in an axial magnetic field of 5–15 T in induction [6], [7], show that, at a time $t \leqslant 5$ ns, an influence of the magnetic field on expansion of the plasma is not observed. For 5 ns, the plasma registered on the level of electron density $n_e = 5 \cdot 10^{17}$ cm^{-3} reaches the distance $z = 1.2$ mm, analogous to the results obtained for $B_0 = 0$. Observation of the plasma in two mutually perpendicular directions allows us to state that the expanding plasma-blob is characterized by high axial symmetry in this period. For $t \leqslant 5$ ns the presence of the magnetic field changes essentially the character of plasma expansion. The plasma, after fast expansion during the first 5 ns, undergoes retardation and, after about 15 ns from the beginning of expansion, reaches the state of mechanical equilibrium with the magnetic field. The axial symmetry of the front part of plasma stream, distinctly apparent at $t = 10$ ns for $z > 0.4$ mm (Fig. 14**a**), gets disturbed. The disturbance of the front of the expanding plasma increases rapidly with time (Fig. 14**b**). Intense deceleration of plasma expansion with the transverse field causes that after 15 ns the plasma attains a state of mechanical equilibrium with the magnetic field. The shape and dimensions of the diamagnetic cavity during the plasma expansion are shown in Fig. 15. After $t = 15$ ns an increase of the diamagnetic cavity is practically stopped. Already in the phase of deceleration of the plasma, a disturbance appears in front of the expanding plasma, clearly evident for $t = 10$ ns (Fig. 15**a**), which enlarges with time. This disturbance is visible during observation of the plasma expansion in two directions simultaneously. Both the mechanism of generation of this disturbance (the deceleration force) as well as the flute character of its development (the disturbances develop along the magnetic field lines) indicate that this is a Rayleigh–Taylor (R–T) instability.

Determining from interferometric measurements the average deceleration of the plasma-blob $g_{\text{eff}} = 3 \cdot 10^{15}$ cm/s^2, and the density length scale $L_n = 0.05$ cm, we can derive the time of development of the R–T instability

$$\tau_{RT} = \sqrt{\frac{L_n}{g_{\text{eff}}}} = 4 \cdot 10^{-9}\ \text{s}. \tag{17}$$

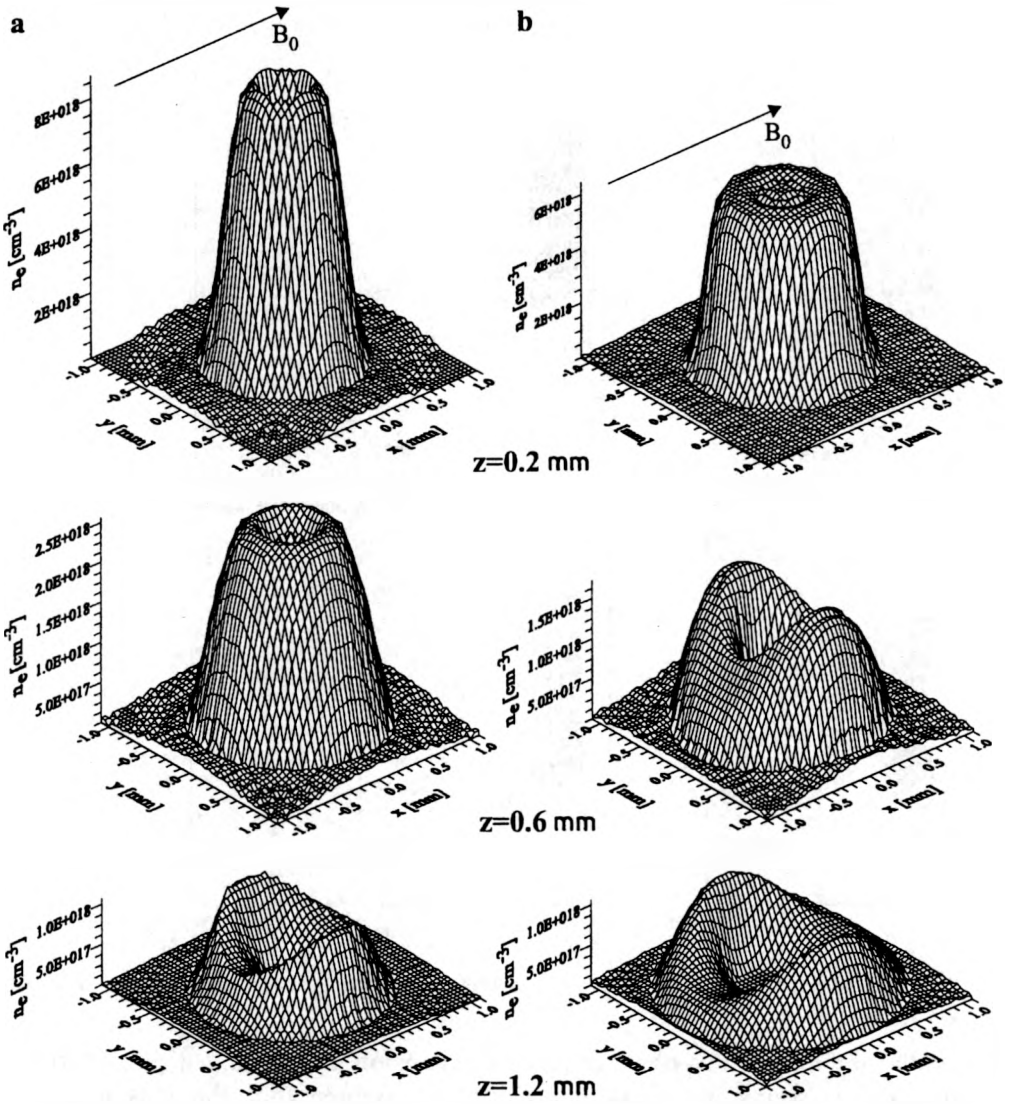

Fig. 14. Electron density distributions in selected "Z" cross-section of plasma ($B_0 = 10$ T), for **a** — $t = 10$ ns, **b** — $t = 15$ ns.

Due to the fact that the Larmor frequency for ions in this period is estimated to be $\omega = 2 \cdot 10^8\ \mathrm{s}^{-1}$, the condition necessary for development of the classical R–T instabilities $\omega_{ci} \cdot \tau_{RT} \gg 1$ is not satisfied. Also the magnitude of the directed ion Larmor radius

$$R_{ld} = \frac{V_0}{\omega_{ci}} = 0.1\ \mathrm{cm}, \tag{18}$$

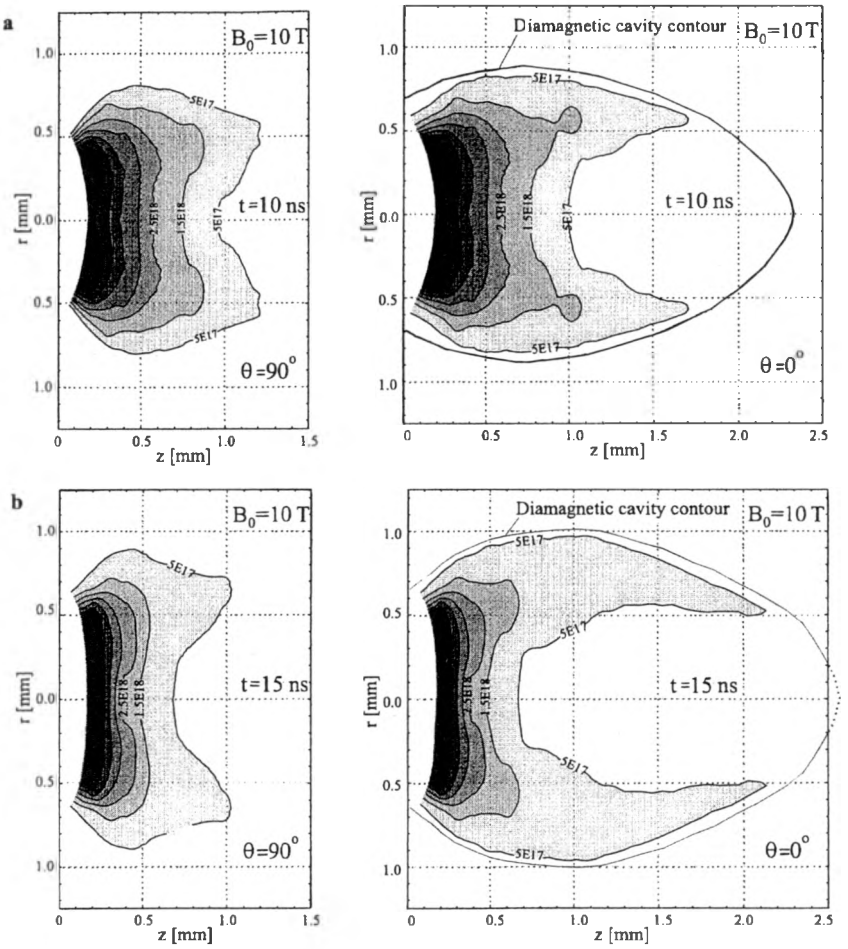

Fig. 15. Spatial distributions of electron density in diamagnetic cavity for two projections: **a** — $t = 10$ ns, **b** — $t = 15$ ns.

proves that the ions in this phase of plasma expansion are unmagnetized. Therefore, in this case, it seems to be more accurate to assume that the reason for the disturbances in the plasma edge is an unmagnetized ion R–T instability [2].

The interferometric measurement presented corresponds with the course of variation in the field $\Delta B^+(t)$, obtained by means of the RMP (Fig. 16). The curve illustrates the process of an increase in the magnetic field during plasma expansion until its stopping which corresponds with the maximum in the plot. Using expansion (13), we have derived the relation for $\rho_{c0}(t)$ illustrating the process of expansion of the diamagnetic cavity (Fig. 17). It results from the $\rho_{c0}(t)$ plot that at $t = 5$ ns the axial dimension of the diamagnetic cavity $\rho_{c0} \approx 1.8$ mm. On the other hand, the plasma edge measurable interferometrically does not exceed 1.3 mm at the moment. This proves that the diamagnetic cavity, in a few first nanoseconds, is created by fast but relatively thin plasma of $n_e < 10^{17}\,\mathrm{cm}^{-3}$. The variations in the velocity of the cavity

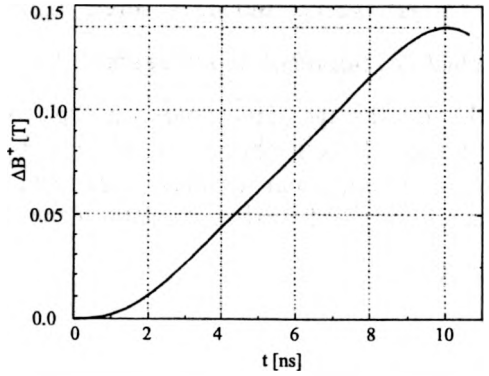

Fig. 16. Variations in the magnetic field during plasma expansion, registered with the RMP method.

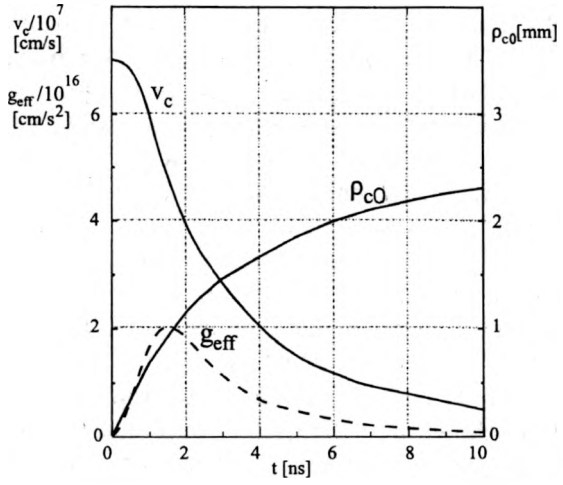

Fig. 17. Plots presenting variations with time of the axial dimension of the diamagnetic cavity ρ_{c0}, and, determined on this basis, variations in the velocity v_c and the deceleration g_{eff} of the cavity.

plasma edge $v_c(t)$ determined on the basis of the $\rho_{c0}(t)$ dependence show that the initial plasma velocity is close to 10^8 cm/s (see Fig. 17). The cavity reaches the maximum dimension $\rho_{c0\,max} = 2.3$ mm, after 10 ns. This corresponds precisely to the axial dimension of the plasma contour at that time moment (see Fig. 15) registered on the level n_e close to $5 \cdot 10^{17}$ cm^{-3}. Thus, it can be stated that for $t \geqslant 10$ ns the shape and dimension of the diamagnetic cavity under investigation can be precisely determined from the interferometric measurements. It results from these measurements that the diamagnetic cavity enlarges slightly with time (see Fig. 15**b**, $t = 15$ ns). The motion of the cavity edge, however, is relatively slow in that period (about 10^6 cm/s) and probably for that reason it is not registered by the magnetic probe. Figure 17 presents also variations in deceleration of the diamagnetic-cavity edge $g_{eff}(t)$. Strong retardation of the plasma in the initial stage of its expansion can be the source of Rayleigh–Taylor instabilities. Taking into account that in the initial

stage of expansion (see Fig. 17) $g_{\text{eff}} \approx 2 \cdot 10^{16}\,\text{cm/s}^2$ we get indeed a small value $\tau_{RT} \approx 1.5$ ns. But since $\tau_{RT} < \frac{2}{\omega_{ci}}$ we can expect fast development of unmagnetized ion instability R–T in the plasma edge already in the initial stage of its expansion. Due to the fact that the plasma at the front of the stream is relatively thin ($n_e < 10^{17}\,\text{cm}^{-3}$), they can be unregisterable interferometrically. Later on, when the plasma concentration on the plasma-magnetic field border increases, the disturbance in the plasma edge should be evident.

5. Conclusions

The results of the interferometric measurements of the laser-produced plasma expansion in the strong axial magnetic field and numerical simulation have shown that the process of mutual interaction of the laser plasma with the magnetic field depends essentially on the character of the target illumination, *i.e.*, the laser-beam intensity distribution in the focal area. It was found that a laser beam having a maximum of its intensity on the axis leads to the angular regime of the plasma expansion whereas the beam with a minimum on the axis leads to the axial one. Despite of the limitation of the physical model used in the numerical code, the results of simulations give a qualitative picture of the phenomenon of the laser plasma flow in an axial magnetic field. Our investigations show that, in axial magnetic field, it is practically impossible to generate a relatively homogeneous stream of a laser-produced plasma in the early phase of plasma expansion, which could be the medium of an X-ray laser. However, it is interesting in this context that a plasma cylinder is created in the final stage of evolution which can constitute an advantageous configuration for propagation and amplification of coherent X-rays.

The interferometric measurements have shown that the transverse magnetic field induces an asymmetry of the plasma distinctly apparent in the interferograms registered in two mutually perpendicular directions. Analysing the spatial and temporal distributions of electron concentration obtained in the transverse magnetic field, it has been proved that the factor responsible for the disturbance of the axial symmetry of the plasma is the Rayleigh–Taylor instability corresponding to the ion unmagnetization state. Fast development of this instability appears in the initial stage of expansion plasma.

Simultaneous application of an interferometry and a non-contact magnetic probe in investigations of plasma expansion in a transverse magnetic field allowed verification of the correctness of the RMP method [11] in the case of strong magnetic fields. It should be emphasized that the cavity dimensions in the equilibrium state obtained with both these methods are exceptionally consistent.

References

[1] DIMONTE G., WILEY L. G., Phys. Rev. Lett. **67** (1991), 1755.
[2] HUBA J. D., HASSAM A. B., WINSKE D., Phys. Fluids B **2** (1990), 1676.

[3] SUCKEWER S., SKINNER CH., VOORHEES D., MILCHBERG H., KEANE C., SEMET A., J. Quantum Electron. **19** (1983), 1855.
[4] PISARCZYK T., KASPERCZUK A., Laser Part. Beams **17** (1999), 313.
[5] PIKALOV V. V., MELNIKOVA T. S., *Niskotemperaturnaya plazma*, t. 13, *Tomografiya plazmy*, "Nauka", Sibirskaya Izd. Firma RAN, Novosibirsk 1995.
[6] PISARCZYK T., BRYUNETKIN B. A., FAENOV A. YA., FARYŃSKI A., FIEDOROWICZ H., KOSHEVOY M. O., MIKLASZEWSKI R., MROCZKOWSKI M., OSIPOV M. V., PARYS P., SKOBELEV I. YU., SZCZUREK M., Phys. Scripta **50** (1994), 72.
[7] KASPERCZUK A., PISARCZYK T., Phys. Scripta **53** (1996), 503.
[8] KASPERCZUK A., MIKLASZEWSKI R., PISARCZYK T., Phys. Scripta **54** (1996), 636.
[9] KASPERCZUK A., PISARCZYK T., J. Tech. Phys. **38** (1997), 521.
[10] PISARCZYK T., ARENDZIKOWSKI R., PARYS P., PATRON Z., Laser Part. Beams **12** (1994), 549.
[11] KASPERCZUK A., PISARCZYK T., ZAKHAROV YU. P., Phys. High Education **4** (1998), 118.
[12] PISARCZYK T., RUPASOV A. A., SARKISOV G. S., SHIKANOV A. S., J. Sov. Laser Res. **11** (1990), 1.
[13] LAPWORTH K. G., ALLNUT L. A., J. Phys.: Sci. Instrum. **10** (1977), 733.
[14] RAIZER YU. P., J. Appl. Tech. Phys. **6** (1963), 19.
[15] ZAKHAROV YU. P., ORISHICH A. M., PONOMARENKO A. G., POSUKH V. G., Sov. J. Plasma Phys. **12** (1986), 674.
[16] ZAKHAROV YU. P., MELEKHOV A. V., NIKITIN S. A., PONOMARENKO A. G., *Diamagnetism of exploding plasma and study of its energy changes on magnetic disturbances in vacuum*, Proc. Intern. Conf. on Plasma Physics, Nagoya, September 9-13, 1996, Vol. II, pp. 1670–1673.
[17] PISARCZYK T., KASPERCZUK A., WOŁOWSKI J., ZAKHAROV YU. P., *Expansion of laser-produced plasma across strong magnetic fields*, Intern. Symp. *Plasma '97, Research and Applications of plasmas*, Jarnołtówek (Poland), June 10–12, 1997, Vol. 1, pp. 171–174.
[18] ZAKHAROV YU. P., [In] 5 Symp. *Double Layers — Potential Formation and Related Nonlinear Phenomena in Plasmas*, [Ed.] World Sci., Singapore 1997, p. 208.

Received November 14, 1999
in revised form January 24, 2000